Available online at www.sciencedirect.com
ScienceDirect
Applied Surface Science 254 (2008) 2146–2149
applied surface science
www.elsevier.com/locate/apsusc

Properties of $Mg_xZn_{1-x}O$ thin films sputtered in different gases

Da-Yong Jiang [a], Ji-Ying Zhang [a,*], Ke-Wei Liu [a], Chong-Xin Shan [a],
Yan-Min Zhao [a], Tong Yang [b], Bin Yao [a], You-Ming Lu [a], De-Zhen Shen [a]

[a] Key Laboratory of Excited State Processes, Changchun Insititute of Optics, Fine Mechanics and Physics,
Chinese Academy of Sciences, Changchun 130033, People's Republic of China
[b] Jilin University, Changchun 130023, People's Republic of China

Received 2 August 2007; received in revised form 30 August 2007; accepted 30 August 2007
Available online 12 September 2007

Abstract

$Mg_xZn_{1-x}O$ alloy films were prepared on sapphire substrates using Ar and N_2 as the sputtering gases. The effect of the sputtering gas on the structural, optical and electrical properties of the $Mg_xZn_{1-x}O$ films was studied. By using N_2 as the sputtering gas, the $Mg_xZn_{1-x}O$ film shows p-type conductivity and the band gap is larger than that employing Ar as the sputtering gas. The reason for this phenomenon is thought to be related to the reaction between N–O or N–Zn, and the N-doping.

Keywords: $Mg_xZn_{1-x}O$; Band gap; Raman; Electrical properties

1. Introduction

Recent advances in the growth of wide band gap semiconducting oxide materials like ZnO have stimulated extensive efforts. Much research has focused on studying the influence of different dopants on their multifunctional properties. These doped oxides exhibit properties that are either enhanced or are entirely new [1–3]. For the practical applications, the band gap engineering is one of the indispensable issues to be achieved, for example, the alloying with magnesium oxide (MgO) to make $Mg_xZn_{1-x}O$ can increase the band gap energy from 3.3 eV for wurtzite ZnO to 7.8 eV for rocksalt MgO with fairly small mismatching (0.1%) in bond lengths of ZnO and MgO [4,5]. With the band gap enlarged compare to binary ZnO, $Mg_xZn_{1-x}O$ alloy has great potential applications in ultraviolet (UV) sensors [6]. However, $Mg_xZn_{1-x}O$ alloys usually show n-type conduction, and it has been proven that fabrication of p-type $Mg_xZn_{1-x}O$ is difficult. Only phosphor doped, nitrogen doped and N–Al co-doped p-type $Mg_xZn_{1-x}O$ alloys have been reported up to now [7-8]. Preparation of stable p-type $Mg_xZn_{1-x}O$ alloy has been a very important issue for ZnO-based UV light-emitting diodes (LED).

Current research on the growth of $Mg_xZn_{1-x}O$ alloys is restricted to pulsed laser deposition (PLD), molecular beam epitaxy (MBE), and magnetron sputtering [9–11]. For using magnetron sputtering method, most reports concentrate on tuning the substrate temperature and the Mg composition in the target to obtain wider band gap $Mg_xZn_{1-x}O$ alloys. To the authors' knowledge, very few reports on the effect of the sputtering gases on the structural, optical and electrical properties of $Mg_xZn_{1-x}O$ alloys, especially on the conduction type of the $Mg_xZn_{1-x}O$ alloys.

Differing from literatures previously reported, $Mg_xZn_{1-x}O$ alloy films have been prepared using magnetron sputtering technique, and the effect of the sputtering gases on the structural and electrical properties of the films has been studied.

2. Experiment

Wurtzite $Mg_xZn_{1-x}O$ alloys were grown on *c*-plane (0 0 2) sapphire substrates with the sputtering gases of Ar and N_2. A $Mg_{0.18}Zn_{0.82}O$ target was prepared by sintering mixture of 99.99 % pure MgO and ZnO powders at 1000 °C for 10 h in air ambient. The distance between the substrates and the target was approximately 20 cm. Prior to deposition, the substrates were

---

* Corresponding author. Tel.: +86 431 86176322; fax: +86 431 85682964.
E-mail address: zhangjy53@yahoo.com.cn (J.Y. Zhang).

0169-4332/$ – see front matter © 2007 Elsevier B.V. All rights reserved.
doi:10.1016/j.apsusc.2007.08.092

cleaned by the standard RCA process. After being loaded into the growth chamber, the substrates temperature was maintained at 400 °C. The working pressure in the chamber was kept at 1 Pa during the film growth. The radio frequency power was kept at 100 W, and the applied voltage was 500 V. The sputtering gases were ultrapure (5N) Ar or N_2 gases, respectively. The gas was introduced into the sputtering chamber through a set of mass flow controllers with the flow rates of 45 sccm (standard cubic centimeter per minute).

The structural properties of the alloy thin films were carried out by X-ray diffraction (XRD) using a D/max-RA X-ray spectrometer (Rigaku) with Cu Kα radiation of 0.154 nm. The surface was examined using scanning electron microscopy (SEM) (Hitachi, S4800). Optical transmission and absorption spectra were recorded using a Shimadzu UV-3101 PC scanning spectrophotometer. Raman spectra were collected with a JY-630 micro-Raman spectrometer. The 325 nm line of a He–Cd laser was employed as the excitation light. Electrical properties were measured in the van der Pauw configuration by a Hall effect measurement system at room temperature.

3. Results and discussion

Fig. 1 shows the XRD spectra near (0 0 2) peak of $Mg_xZn_{1-x}O$ films deposited under different sputtering gases. The samples sputtered in Ar and N_2 are defined as samples (a) and (b), respectively. It is observed that both films have wurtzite structure. The full width at half maximum (FWHM) of sample (a) (0.39°) is smaller than sample (b) (0.67°). The shrinkage in FWHM shows that sample (a) has lower defects than sample (b) which can be partly confirmed by the SEM images in Fig. 1(a′ and b′). Furthermore, the *c*-axis lattice constant of samples (a) and (b) were evaluated to be 5.168 and 5.135 Å, respectively, which are smaller than the value of 5.209 Å of ZnO powder sample [12]. The decrease of the *c*-axis lattice constant implies some Mg atoms have substituted Zn in the films. Therefore, we supposed that the Mg composition of sample (a) is smaller than sample (b), which is confirmed by the energy dispersive spectroscopy (EDS) data shown in Fig. 2. C signals can be observed in both spectra which may come from the organic solvents used in the substrate cleaning process. Furthermore, N signals are observed in Fig. 2(b).

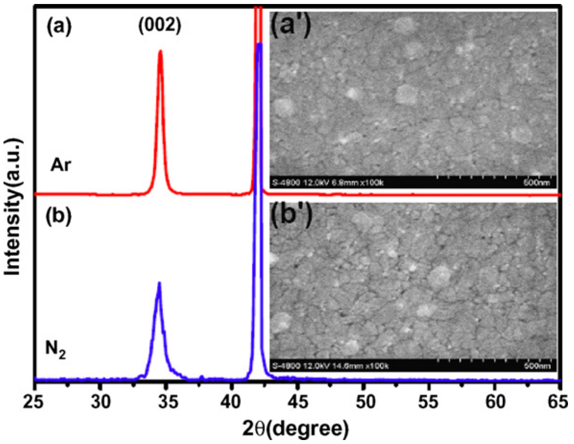

Fig. 1. XRD patterns of $Mg_xZn_{1-x}O$ alloy films prepared under Ar ambient (a) and N_2 ambient (b). The inset (a′) and (b′) are the SEM images of samples (a) and (b).

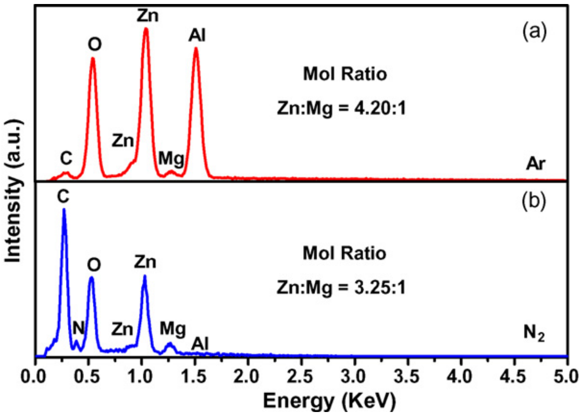

Fig. 2. EDS of samples (a) and (b).

To investigate the optical properties of the $Mg_xZn_{1-x}O$ thin films, the room temperature transmission spectra were measured in the range from 200 to 600 nm, as shown in Fig. 3. Both samples exhibit sharp absorption edge. It is noted that no significant variation in transmission is observed in the visible range under different sputtering gases. The absorption edge shifts to the lower wavelength sputtered in N_2 ambient compared with that in Ar ambient.

In order to observe the band gap variation of two samples, the method of calculate the band gap can be expressed as the formula [13]:

$$\alpha^2 = \left(\frac{A}{h\upsilon}\right)^2 (h\upsilon - E_g)$$

where α is the absorption coefficient, A a constant, and $h\upsilon$ is photon energy. The band gap energy (E_g) can be obtained by plotting $(\alpha h\upsilon)^2$ versus $h\upsilon$ and linear extrapolation to $\alpha = 0$. Fig. 4 shows the plot of $(\alpha h\upsilon)^2$ as a function of photon energy ($h\upsilon$). The band gap of sample (b) (3.63 eV) is larger than that of sample (a) (3.38 eV). For $Mg_xZn_{1-x}O$ alloys, the band gap is determined by the Mg composition in the alloy films.

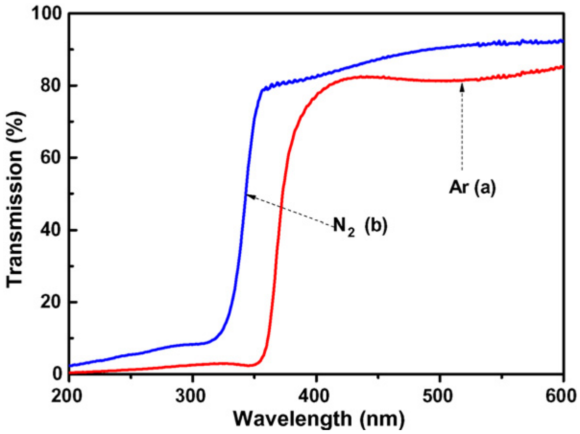

Fig. 3. Transmission spectra of samples (a and b).

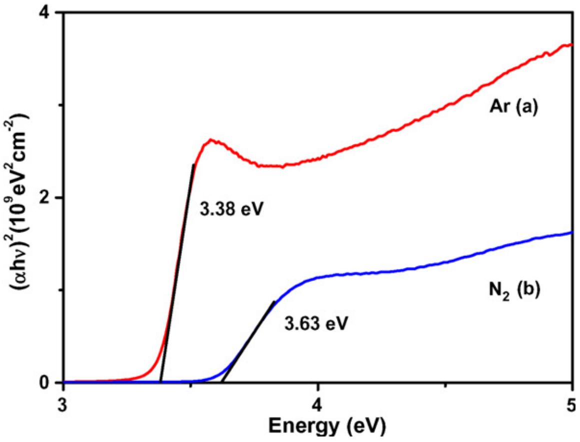

Fig. 4. Variations of $(\alpha h\upsilon)^2$ vs. $h\upsilon$ for samples (a and b).

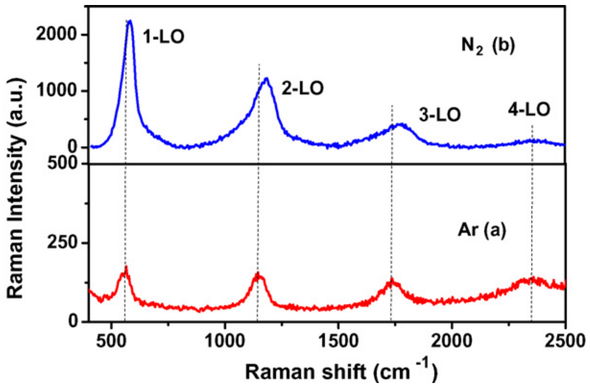

Fig. 5. Room temperature Raman spectra of samples (a and b).

Obviously, Mg composition in sample (a) is smaller than sample (b). This reason is attributed to the different sputtering gases. We propose that there are two reasons for Mg-rich in sample (b). First, it is known that some Mg, Zn and O atoms escape from the $Mg_xZn_{1-x}O$ target in a state of atom or ion when the target is sputtered by the Ar or N_2 plasma. If Ar is used ad the sputtering gas, Ar atoms or ions will react hardly. However, if N_2 is the sputtering gas, the O atoms or ions will react with N atoms and ions produced by ionization of the N_2 gas to form NO or NO_2, which will be expelled from the growth chamber by pump soon. This reaction results in the fact that the O atoms or ions decrease in the chamber and the (Mg, Zn) to O ratio is much larger than the stoichiometric ratio of 1:1. That is, there are many excessive Mg and Zn atoms. Since the bond energy of Mg–O is larger than that of Zn–O, some of Zn atoms will react with O atoms or ions hardly and these unreacted excessive Zn atoms will not deposit on the substrate due to re-evaporation induced by the lack of O atoms or ions and the high substrate temperature. Second, the band gap shifted to the higher energy side partly due to the Zn–N bond formation, which cannot be neglected. The Zn–N bond formation can be confirmed by N-doped ZnO film [14]. Due to the Zn–N bond formation, part of Zn atoms were not at the normal lattice points, that will result in Mg-rich condition in the film. However, N atom has larger atomic radius than O atom. Thus the bond energy of Zn–N is smaller, which can be replaced by Zn–O bonds. So the amount of Zn–N bond will be less. We deem that the Zn–N bond formation is not the main reason for the blueshift. But the cracks of the inset (b′) of Fig. 1 can be partly attributed to the formation of ZnN. As a result, Mg composition in sample (b) is larger.

Raman scattering spectra of the samples are collected in a backscattering geometric configuration at room temperature. The two samples show intense multiphonon scattering in the range from 400 to 2500 cm^{-1}. Fig. 5 shows typical resonant Raman scattering spectrum of two samples, which are composed of four sharp lines at wavenumbers that are multiples of the 1-longitudinal optical (LO) zone-center frequency. As can be seen from Fig. 5, each order LO of sample (b) shifted to the higher frequency in comparison with sample (a), indicating that there are more Mg atoms in sample (b) than (a). Compared with sample (a), the 1-LO frequency of sample (b) shows a significant broadening. It is supposed that there are many new defects which are induced by Mg and N atoms.

Table 1
Conductivity type, carrier mobility, resistivity, and carrier concentration of samples (a and b)

MZO sputtering gas	Type	Mobility ($cm^2\,V^{-1}\,s^{-1}$)	Resistivity (Ω cm)	Concentration (cm^{-3})
Ar	n	2.1	3.2×10^3	5.0×10^{16}
N_2	P	0.1	5.6×10^4	6.1×10^{15}

Hall measurements indicate that the two samples have different conduction type. Metal Indium was used for the Ohm contact with $Mg_xZn_{1-x}O$ films and their electrical parameters are listed in Table 1. As mentioned above, the fabrication of p-type $Mg_xZn_{1-x}O$ is hard to achieve. Sample (a) shows n-type conductivity, implying that it has many native donor defects, such as O vacancies (V_O) and Zn interstitial (Zn_i). However, by using N_2 as the sputtering gas, sample (b) exhibits p-type conductivity due to compensating these native donor defects. The p-type conductivity is related to N doping. We deduce that it is formed by substitution of N atom for O sublattice to act as an acceptor. The reason for the similar result has been analysed with N-doped Mg–Zn–O film [15]. This also implies that the acceptor about N-doped has a negligible effect on the crystal quality of the alloy film.

4. Conclusions

Wurtzite $Mg_xZn_{1-x}O$ thin films were prepared by magnetron sputtering using Ar and N_2 as the sputtering gases on Al_2O_3 substrates. By using N_2 as the sputtering gas, due to the reaction between N–O and N–Zn during sputtering process, this results in that Mg will be rich. Compared with Ar as the sputtering gas, the band gap will be widen. Although the crystal quality of the alloy film will decrease, p-type conductivity of the alloy was obtained, which is related to N-doping.

Acknowledgments

This work is supported by the key Project of National Natural Science Foundation of China under Grant No.

60336020, No. 50532050, the Innovation Project of Chinese Academy of Sciences. The National Natural Science Foundation of China under Grant No. 60429403, No. 10674133 and No. 60506014.

References

[1] A. Ohtomo, M. Kawasaki, T. Koida, K. Masubuchi, H. Koinumpa, Y. Sakurai, Y. Yoshida, T. Yasuda, Y. Segawa, Appl. Phys. Lett. 72 (1998) 2466.

[2] P. Sharma, A. Gupta, K.V. Rao, F.J. Owens, R. Sharma, R. Ahuja, B. Johansson, G.A. Gehring, Nat. Matter 2 (2003) 673.

[3] T. Makino, Y. Segawa, M. Kawasaki, A. Ohtomo, R. Shiroki, K. Tamura, T. Yasuda, H. Koinuma, Appl. Phys. Lett. 78 (2001) 1237.

[4] W. Yang, R.D. Vispute, S. Choopun, R.P. Sharma, T. Venkatesan, H. Shen, Appl. Phys. Lett. 78 (2001) 2787.

[5] W.R.L. Lambrecht, S. Limpijumnong, B. Segall, MRS Internet, J. Nitride Semicond. Res. 4S1 (2000) G 6.8.

[6] Y. Yang, S.S. Hullavard, B. Nagaraj, I. Takeuchi, R.P. Sharma, T. Venkatesan, R.D. Vispute, H. Shen, Appl. Phys. Lett. 82 (2003) 3424.

[7] Y.W. Heo, Y.W. Kwon, Y. Li, S.J. Pearton, D.P. Norton, Appl. Phys. Lett. 84 (2004) 3474.

[8] X. Zhang, X.M. Li, T.L. Chen, C.Y. Zhang, W.D. Yu, Appl. Phys. Lett. 87 (2005) 092101.

[9] S. Choopun, R.D. Vispute, W. Yang, R.P. Sharma, T. Venkatesan, H. Shen, Appl. Phys. Lett. 80 (2002) 1529.

[10] K. Ogata, K. Koike, T. Tanite, T. Konuro, F. Yan, S. Sasa, M. Inoue, M. Yano, J. Cryst. Growth 251 (2003) 623.

[11] M. Takashi, N. Takayuki, N. Shiro, H. Takakura, Y. Hamakawa, Thin Solid Films 372 (2000) 173.

[12] C. Suryanarayana, M.G. Norton, X-Ray Diffraction: A Practical Approach, 1998, p. 263.

[13] J.M. Pawlikowski, Phys. Rev. B 26 (1982) 4711.

[14] J.G. Ma, Y.C. Liu, R. Mu, J.M. Zhang, Y.M. Lu, D.Z. Shen, X.W. Fan, J. Vac. Sci. Technol. B 22-1 (2004) 94.

[15] Z.P. Wei, B. Yao, Z.Z. Zhang, Y.M. Lu, D.Z. Shen, B.H. Li, X.H. Wang, J.Y. Zhang, D.X. Zhao, X.W. Fan, Z.K. Tang, Appl. Phys. Lett. 89 (2006) 102104.